chemical nature of the adsorbant/adsorbed system. The same conclusion may be drawn from the comparison of the data referring to the copper-oxygen and silver-oxygen systems, the values for the thickness decrease being in agreement with the chemical properties of the two metals.

Table 2 contains the values of the thickness decrease, δ', computed from the resistance increase by assuming not only a thickness variation but also a change in the number of conduction electrons (*5*, *9*).

TABLE 2
δ'-VALUES

Adsorbant/adsorbed system	δ'(Å) (*9*, *5*)
Cu/O_2	5.91 ± 0.46
Ag/O_2	3.08 ± 0.24

As it may be noticed this assumption affects neither the magnitude order nor the specific character of the thickness decrease. In other words, even by yet admitting another mechanism for the interpretation of the resistance variation in thin metallic films during oxygen chemisorption, Sachtler and Dorgelo's hypothesis remains valid.

REFERENCES

1. MURGULESCU, I. G., COMSA, GERDA H., AND IONESCU, N. I., *J. Catalysis* **12**, 102 (1968).
2. SACHTLER, W. M. H., AND DORGELO, G. J. H., *Z. Physik. Chem.* (Frankfurt) **25**, 69 (1960).
3. MURGULESCU, I. G., AND IONESCU, N. I., *Rev. Roumaine Chim.* **11**, 1035 (1966).
4. MURGULESCU, I. G., AND COMSA, GERDA, *Rev. Roumaine Chim.* **13**, 1261 (1968).
5. MURGULESCU, I. G., AND IONESCU, N. I., *Rev. Roumaine Chim.* **11**, 1267 (1966).
6. MURGULESCU, I. G., AND IONESCU, N. I., *Rev. Roumaine Chim.* **13**, 1533 (1968).
7. MURGULESCU, I. G., AND COMSA, GERDA, *Rev. Roumaine Chim.* **11**, 1253 (1966).
8. MURGULESCU, I. G., AND COMŞA, GERDA, *Rev. Roumaine Chim.* **12**, 1171 (1967).
9. MURGULESCU, I. G., AND IONESCU, N. I., *Rev. Roumaine Chim.* **14**, (1969) (in press).
10. COMŞA, GERDA, *Rev. Roumaine Chim.* **13**, 1003 (1968).
11. MOELWYN-HUGHUES, E. A. *in* "Physical Chemistry" (2nd revised edition) p. **644**. Pergamon, 1964.

I. G. MURGULESCU
N. I. IONESCU
GERDA H. COMŞA

Institute of Physical Chemistry
Academy of the Sociaist Republic of Romania
Bucharest 9, str. Dumbrava Rosie 23
Romania

Received October 22, 1968

Cage Effect on Product Distribution from Cracking over Crystalline Aluminosilicate Zeolites

Previous publications (*1*, *2*) described the hydrocarbon cracking activity of various zeolites for *n*-hexane. Zeolite catalysts have been shown to have one to more than four orders of magnitude higher activity than that of conventional cracking catalysts.

With these zeolites it is possible to carry out hydrocarbon cracking reactions at temperatures considerably below the conventional cracking temperatures of ~500°C. As previously noted, temperature has a pronounced effect on product pattern in hexane cracking (*2*). The products are rich in C_4–C_5 at 316°C (600°F), and due to secondary reactions they shift toward predominantly C_3 hydrocarbons at 480°C (900°F).

Of particular interest is the study of the primary product pattern from cracking with shape-selective zeolites. It has previously been shown that when cracking

n-hexane, over these materials, only straight-chain cracked products are observed (*2*, *3*). Any branched molecules formed within the intracrystalline volume are unable to pass out through the interconnecting channels into the bulk phase.

We now report on a series of low-temperature (250–400°C) vapor-phase cracking experiments involving n-paraffins of varying chain length ranging from n-decane to n-hexatriacontane, over a shape-selective zeolite, erionite* (*2*).

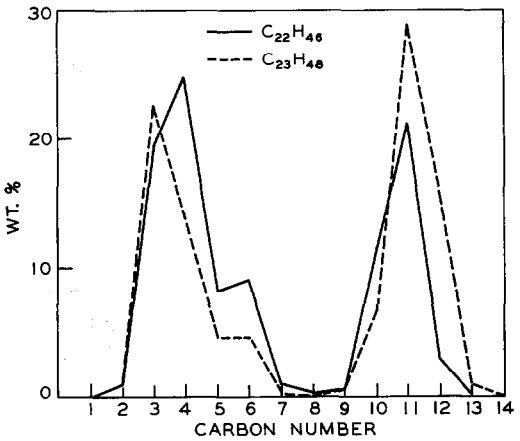

FIG. 1. Carbon number distribution of cracked products over erionite at 340°C.

These experiments were conducted in a fixed-bed microreactor containing a 5-cc preheater section filled with Vycor chips and a 0.5 to 1.5 cc 30/60 mesh catalyst bed. The hydrocarbon was introduced into the microreactor via a syringe pump together with a stream of helium such that the reactant partial pressure was about 100 mm Hg and the superficial contact time was 1 to 3 sec [superficial catalyst volume/gaseous volume (STP) flow rate]. The reaction was continued for a period of 10 min, during which time the product was collected in a liquid nitrogen bath. Then, after desorbing the catalyst with helium for an additional 10 min, the amount of "coke" deposited on the catalyst was determined by converting the carbon to CO_2 and measured volumetrically and a total material balance was made. Conversion was generally between 5% and 30%.

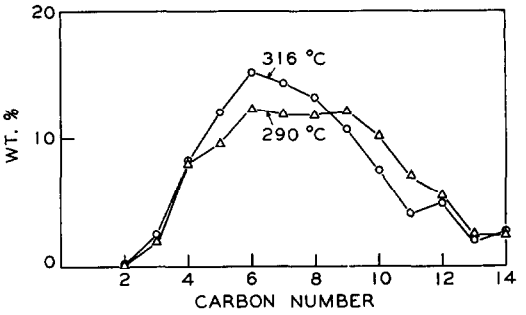

FIG. 2. Carbon number distribution of cracked products over rare earth-exchanged zeolite X.

We find an unusual product pattern when cracking n-docosane (n-$C_{22}H_{46}$) over erionite. Products in the carbon number range of C_1–C_2, C_7–C_9, and $>C_{12}$ are missing, suggesting stepwise and consecutive C–C scission reactions of the type $C_n \rightarrow C_{n/2} \rightarrow C_{n/4}$, etc. The carbon number distribution of the cracked products exhibited a trimodal pattern with peaks at C_{11}, C_6, and C_{3-4}, respectively, as shown in Fig. 1.

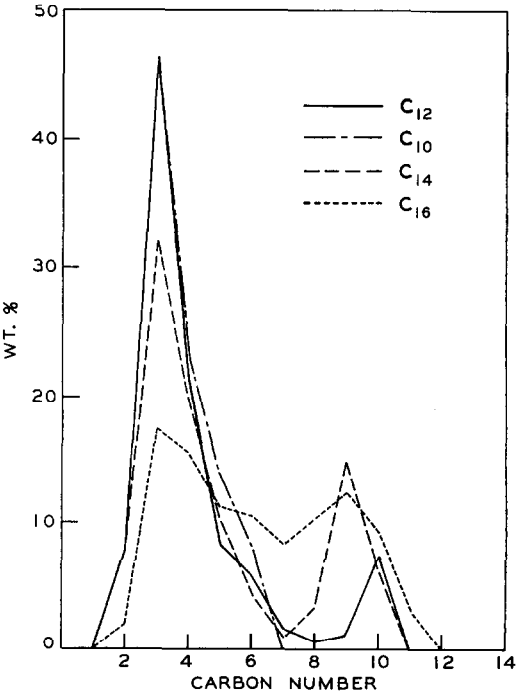

FIG. 3. Product pattern over erionite at 316°C.

*Before recent clarification of the structural difference between erionite and offretite (*4*) the two names were used as synonyms in our earlier publication (*2*).

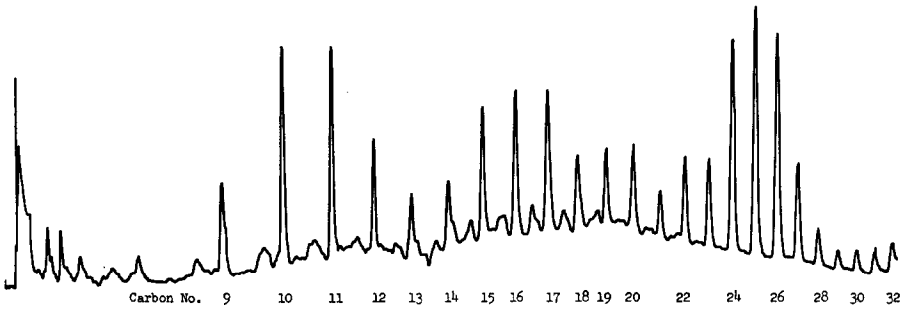

FIG. 4. Chromatogram of condensed product from cracking n-$C_{36}H_{74}$ over erionite at 400°C.

Also shown in Fig. 1 is the result from n-tricosane (n-$C_{23}H_{48}$). Here we noticed that the primary cracked products are in the C_{11}–C_{12} range.

The shift toward "center" cracking with decreasing temperature is generally observed over zeolite catalysts. An example of this is illustrated by the cracking of n-docosane over a rare earth-exchanged X-type zeolite prepared according to ref. (*5*). As shown in Fig. 2, a shift toward C_{11}, as the reaction temperature was lowered, was clearly demonstrated. However, the carbon number distribution resembles the normal pattern expected from the carbonium ion mechanism, with no breaks in any carbon number range.

To demonstrate that the selectivity for C_{10}–C_{12} products was not simply the result of "center cracking" we performed the following experiment: n-decane (n-$C_{10}H_{22}$), n-dodecane (n-$C_{12}H_{26}$), and n-tetradecane (n-$C_{14}H_{30}$) were cracked over erionite. As shown in Fig. 3, even with these smaller molecules, a similar product pattern is observed, although C_9–C_{10} rather than C_{10}–C_{12} were the predominant products.

Another such example is illustrated by the cracking of n-hexatriacontane (n-$C_{36}H_{74}$) over erionite. A chromatogram of the condensed product is reproduced in Fig. 4. It is interesting to note that between C_9 and C_{32} there are three groups of high peaks, namely C_{10}–C_{11}, C_{15}–C_{17}, and C_{24}–C_{26}, respectively, with relatively small peaks in between. These high peaks correspond approximately to the successive scission of C_9–C_{11} fragments from long-chain molecules.

However, in the cracking of n-hexadecane (n-$C_{16}H_{34}$) over erionite, significant amounts of C_7 and C_9 products were found. As shown in Fig. 3, the trimodal pattern is less pronounced and resembles that obtained with a large-pore zeolite (Fig. 2).

The difference in product distribution between large-pore zeolites and the small-pore erionite led us to examine the possible influence of structural factors on product selectivity. We shall designate this as a cage or window effect. The structural considerations may be briefly summarized as follows: erionite crystals may be visualized as hexagonal cylinders partitioned lengthwise along the cylindrical axis by six-membered oxygen rings (2.5-Å free diameter) into cylindrical cavities each 15.1 Å long (12.9 Å free height) (*6*). The six-membered oxygen rings are too small to allow direct passage of hydrocarbon molecules along the cylindrical axis (*7*). These hexagonal cylinders are bundled together with interconnecting windows of eight-membered oxygen rings on the wall of the cylinders. These windows provide the intracrystalline passage for hydrocarbon molecules. The calculated path length over which a hydrocarbon molecule could travel between two nearest windows is 15.4 Å, or if the terminal oxygen atoms are included, 18.2 Å. The lengths of C_{10}–C_{12} n-paraffins (15.3, 16.6, and 17.9 Å, respectively) nearly equal this distance. This suggests that C_{10}–C_{12} fragments, which can bridge across two windows, preferentially pass through the crystal unchanged, while those in the C_7–C_9 and $>C_{12}$ range undergo secondary reactions and do not appear in the product.

Our catalytic data suggest that the unusual product patterns observed could be attributed to this cage effect superimposed on the conventional cracking mechanism.

REFERENCES

1. WEISZ, P. B., AND MIALE, J. N., *J. Catalysis* **4**, 529 (1965).
2. MIALE, J. N., CHEN, N. Y., AND WEISZ, P. B., *J. Catalysis* **6**, 278 (1966).
3. WEISZ, P. B., AND FRILETTE, V. J., *J. Phys. Chem.* **64**, 382 (1960).
4. BENNETT, J. M., AND GARD, J. A., *Nature* **214**, 1005 (1967).
5. PLANK, C. J., ROSINSKI, E. J., AND HAWTHORNE, W. P., *Ind. Eng. Chem. Prod. Develop.* **3**, 165 (1964).
6. STAPLES, L. W., AND GARD, J. A., *Min. Mag.* **32**, 261 (1959).
7. BARRER, R. M., AND KERR, I. S., *Trans. Faraday Soc.* **55**, 1915 (1959).

N. Y. CHEN
S. J. LUCKI
E. B. MOWER

Mobil Research and Development Corp.
Research Department
Paulsboro Laboratory
Paulsboro, New Jersey 08066
Received October 17, 1968;
revised December 9, 1968

Infrared Studies of Hydroxyapatite Catalysts

Adsorbed CO_2 2-Butanol and Methyl Ethyl Ketone

Previous infrared investigations of primary alcohols adsorbed on alumina (*1–4*) have been interpreted as follows: in addition to physically adsorbed alcohol, a chemisorbed species with an alkoxide structure is formed at low temperatures, and it has been suggested that the molecules are cleaved by the dual acid–base sites in a manner analogous to rehydration of the surface (*5*); ammonia has been shown to react in this way (*6*); at higher temperatures the alkoxide species is converted into a surface carboxylate (*1*), and H_2 appears in the gas phase (*2*). Although alumina is not a catalyst for dehydrogenation, the carboxylate species could be interpreted as a dehydrogenation intermediate too stable to desorb as product aldehyde. It is the purpose of the present communication to show that these same infrared bands appear with slight modification when 2-butanol is adsorbed on hydroxyapatite catalysts.

In the course of our experiments, infrared bands attributable to bound carbonate were found, and studies were made to ascertain whether CO_2 might have been incorporated into the surface in a manner similar to the formation of the carboxylate species.

Three catalyst preparations were studied. The first of these was a stoichiometric hydroxyapatite (Ca/P = 1.67), which was active for both dehydrogenation and dehydration of alcohols; the others were nonstoichiometric preparations (Ca/P = 1.58 and 1.63), which were active for dehydration only (*7*). The properties of these materials and the procedures used in their preparation are detailed elsewhere (*8*). Infrared spectra were obtained with a Beckman IR-12 spectrometer from pressed wafers mounted in a cell which could be heated to elevated temperatures (*9*).

The infrared spectra of the parent catalysts (Fig. 1) contained bands in the 1400- to 1500-cm^{-1} region which have been attributed to bound carbonate (*11*). While these bands were weak relative to the P–O vibrational bands, they increased monotonically with the Ca/P ratio, and small shifts in wavelength and relative intensity were recorded. Although the double peak could be attributed to the presence of a basic, rather than a simple, carbonate (*11*, *12*), it has been observed in natural apatites where it has been interpreted (*10*) as either a splitting of the ν_3 vibration of CO_3^{2-} in an environment of low symmetry or as CO_3^{2-} in